Ecotoxicology and Environmental Safety 234 (2022) 113365

Contents lists available at ScienceDirect

Ecotoxicology and Environmental Safety

journal homepage: www.elsevier.com/locate/ecoenv

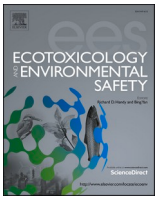

Antioxidant response to heavy metal pollution of regi lagni freshwater in *Conocephalum conicum* L. (Dum.)

Viviana Maresca [a], Giovanna Salbitani [a], Federica Moccia [b], Piergiorgio Cianciullo [a], Federica Carraturo [a], Sergio Sorbo [c], Marilena Insolvibile [d], Simona Carfagna [a], Lucia Panzella [b], Adriana Basile [a,*]

[a] Department of Biology, University of Naples Federico II, Naples, Italy
[b] Department of Chemical Sciences, University of Naples Federico II, Naples, Italy
[c] CeSMA, section of Microscopy, University of Naples Federico II, Naples, Italy
[d] ISPRA, Italian National Institute for Environmental Protection and Research, Rome, Italy

ARTICLE INFO

Keywords:
Conocephalum conicum
Bryophyta
Heavy metal pollution
Oxidative stress and antioxidant responses
Polyphenol
Glutathione

ABSTRACT

Conocephalum conicum L. is a cosmopolitan liverwort species able to respond to local environmental pollution by changing its biological features. In the present study, we assessed the different biological responses in *C. conicum* to heavy metal contamination of Regi Lagni channels, a highly polluted freshwater body. As for the in field experiment, we set up moss bags containing collected samples of the local wild growing *C. conicum*, from the upstream site (non-polluted area), and we exposed them in the three selected sites characterized by different and extreme conditions of heavy metal pollution. In addition, to better understand the contribution of heavy metals to the alterations and response of the liverwort, we performed *in vitro* tests, using the same concentration of heavy metals measured in the sites at the moment of the exposition. In both experimental settings, bio-accumulation, ultrastructural damage, reactive oxygen species production and localization, antioxidant enzymes activity (superoxide dismutase, catalase and glutathione S-transferases), glutathione (reduced and oxidized) levels, localization of compounds presenting thiol groups and phenolic content were investigated. The results showed that the samples from different sites and conditions (for *in vitro* tests) showed significant differences. In particular, the ultrastructural alterations show a trend correlated to the different exposure situations; ROS contents, glutathione, antioxidant enzyme activities, and phenolic contents were increased showing an enhancement of the antioxidant defense both by the enzymatic way and by using the synthesis of antioxidant phenolic compounds. This study confirms the ability of *C. conicum* to respond to heavy metal pollution and the responses studied are, at least partially, correlated to the presence of heavy metals. All the responses considered respond consistently with the pollution trend and they can be proposed as pollution biomarkers. Therefore, we suggest the use of *C. conicum* to identify local hot spots of pollution in further investigation.

1. Introduction

The Regi Lagni channels are a drainage and canalization work done during the Bourbon regency in the early 1600 s in the former Kingdom of Two Sicily. The channels were constructed to avoid the flooding of the ancient Clanius river that affected the nearby territories. The Regi Lagni network is constituted by mostly artificial straight channels, branching through a highly-populated area (2796,360 inhabitants) of about 1905 km^2 comprising the provinces of Caserta, Avellino, Naples, and Benevento. Nowadays, Regi Lagni channels are affected by severe pollution due to the heavy urbanization and industrialization of the surrounding areas, collecting wastewaters and carrying them from the plain north of Naples to the Tyrrhenian Sea (di Martino, 2014; Bove et al., 2011; Grezzi et al., 2011). Furthermore, the network crosses areas such as "Land of Fire" and the "Triangle of Death" which are notorious for the high degree of environmental risk associated with soil and groundwaters due to

* Corresponding author.
E-mail addresses: viviana.maresca@unina.it (V. Maresca), giovanna.salbitani@unina.it (G. Salbitani), federica.moccia@unina.it (F. Moccia), piergiorgio.cianciullo@unina.it (P. Cianciullo), federica.carraturo@unina.it (F. Carraturo), sersorbo@unina.it (S. Sorbo), marilena.insolvibile@isprambiente.it (M. Insolvibile), simcarfa@unina.it (S. Carfagna), panzella@unina.it (L. Panzella), adbasile@unina.it (A. Basile).

https://doi.org/10.1016/j.ecoenv.2022.113365
Received 14 January 2022; Received in revised form 25 February 2022; Accepted 27 February 2022

illegal waste dumping and the soot fallout from uncontrolled garbage burning (Basile et al., 2009; Maresca et al., 2020b; Sorbo et al., 2008). Environmental pollution is the main health risk in Europe and is associated with heart disease, stroke, lung disease and lung cancer in the local population (Senior and Mazza, 2004). The need is therefore felt to implement monitoring practices in order to obtain information on the quality of the environment. Bryophytes are frequently used for biomonitoring purposes both as bioindicators and as accumulators of pollutants, especially heavy metals.

For biomonitoring purposes, we choose three sites along with the Regi Lagni Channels. The former (upstream site), representative of the unpolluted section of the channels, is located in Avella; the other two representatives of areas with the strong environmental pollution in Acerra and Castel Volturno respectively. We collected samples of the local wild growing bryophyte vegetation, being bryophytes well-knows pollution bioindicators and/or bio accumulators, and we choose *Conocephalum conicum* L. (Dum.) (Marchantiales, Bryophyta), which among the bryophytes present showed the most extensive presence, as a species to be used for our study. The *C. conicum* can grow both on humid soils and along the edges of watercourses. Along the Regi Lagni freshwater, the liverwort has been found wild-growing abundantly on the banks of the upstream site. Previous studies reported that this species was able to respond to local environmental pollution and /or heavy metal treatment by changing its ultrastructure and other biological features as Heat Shock Proteins 70 content (Basile et al., 2013).

The present study aims to investigate oxidative stress responses induced by heavy metal pollution in the Regi Lagni watercourse on *C. conicum* exposed in bags in three sites characterized by different environmental conditions. In addition, to evaluate the exact role of heavy metals in inducing the effects studied, a parallel *in vitro* study was conducted, in which the same concentrations of heavy metals, measured in water at the time of exposure, were tested.

In particular, in this study the levels of heavy metals in the surveyed sites were measured in order to determine their degree of pollution. Subsequently, various analyzes were carried out on *C. conicum* samples both exposed in field and cultivated *in vitro*. Bioaccumulation of heavy metals in the gametophyte, the activity of antioxidant enzymes (superoxide dismutase, catalase and gluathione peroxidase), quantification and localization of reactive oxygen species, ultrastructural damage, localization of compounds presenting thiol groups, reduced/oxidized glutathione ratio, synthesis of polyphenols, compounds known to be valid antioxidants, were measured.

2. Materials and methods

2.1. Plant material

Samples of *C. conicum* were collected from upstream of the channel of the Regi Lagni (non-polluted area), identified by prof. Adriana Basile. A sample was deposited in the herbarium of the Botanical Garden of the University Federico II Napoli. The collected samples were used for both the in-field and *in vitro* experiments.

2.2. In field experiments

After collection, about 1.8 g (FW) of homogeneous samples of *C. conicum* thalli were rinsed with MilliQ Water and wrapped with > 49 mm^2 - meshed nylon bags, as described in Kelly et al. (1987). For each site six samples were exposed for seven days in April 2019. In order to avoid submersion thalli were exposed at a water depth of 1 cm.

The coordinates of the 3 selected sites are reported in Maresca et al. (2018) (Fig. 1S). Three exposure sites with different pollution degrees were chosen: (A) Avella, as pristine site, (B) Acerra, (C) Castel Volturno, as representative of the highly polluted areas: the "Triangle of Death" and "Land of Fires", respectively.

Samples from each site were merged and then splitted into three subsamples for the subsequent analyses. Water was sampled three times in each site on the day of the *C. conicum* exposure and then it was analysed for heavy metal concentration.

2.3. In vitro experiments

The samples collected from upstream of the channel of the Regi Lagni (non-polluted area), have been rinsed with MilliQ Water and cultured in

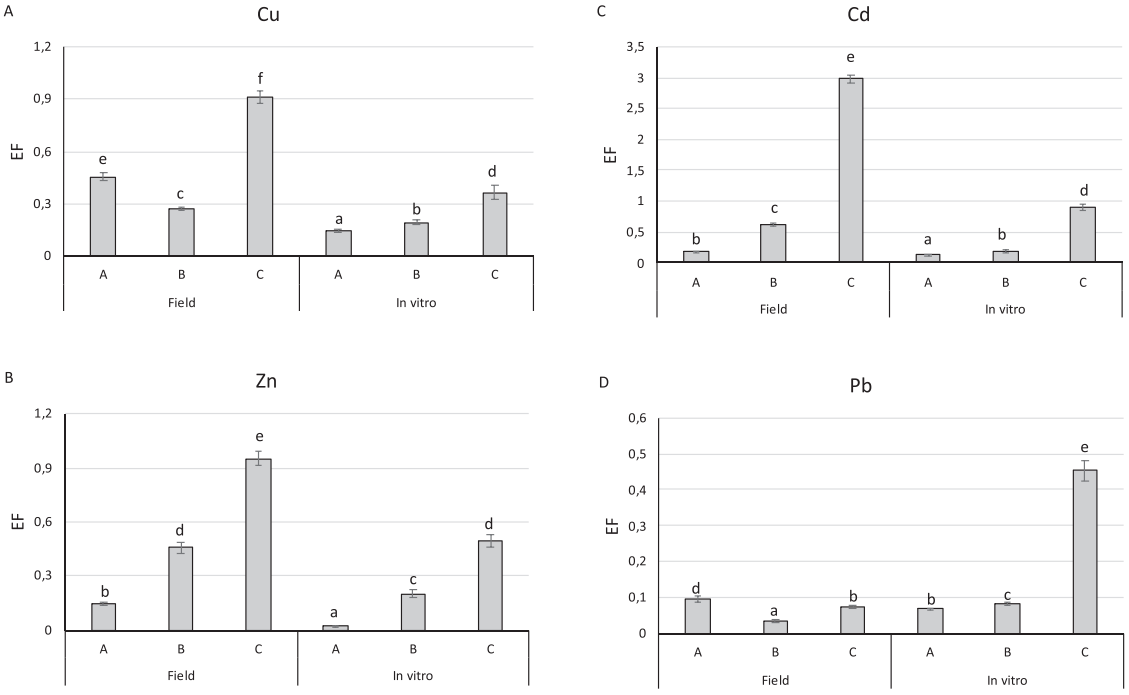

Fig. 1. Enrichment Factor (EF) of heavy metals in the field and *in vitro* experiments. Values are presented as mean ± st. dev; bars not accompanied by the same letter are significantly different at $P < 0.05$, using the post-hoc Student–Newman–Keuls test.

Petri dishes (10 cm diameter), 20 specimens per dish, using sterile modified Mohr medium, pH 7.5 as reported in Esposito et al. (2012) and in the same medium with the addition of the metal salts.

The cultures were kept for seven days in a climatic chamber and the environmental parameters were set based on the environmental conditions recorded in the field [air temperature: at 22 ± 1.4 °C, and 14 ± 1.4 °C, mean ± SD, during day and night, respectively; relative humidity: 71 ± 3% mean ± SD, 16 h light (Photosynthetic Active Radiation 400 μmol m^2 s^{-1})/8 h dark photoperiod]. In the cultures, were added to the medium the metals as soluble salts: $CdCl_2$, $CuSO_4$, Pb $(CH_3COO)_2$, and $ZnCl_2$ with the relative anions as K salts in control solutions.

The concentration of heavy metals used in the *in vitro* samples was the same measured in the three surveyed sites. The samples are indicated as follows:

– Ctrl, A, B, C, for both field and *in vitro* samples;.

The *in vitro* and in field samples were performed in triplicate and repeated three times.

2.4. Analytical determination of metal in water samples and in liverwort

Heavy metals were determined in both water samples (from in-field experiments) and liverwort (in field and *in vitro* experiments). The water samples collected in the field experimental sites were analyzed by ICP-MS (Perkin-Elmer Sciex 6100) for the concentration of selected heavy metals: Cd, Cu, Pb, Zn as described in Maresca et al. (2018).

After both in the field and *in vitro* experiments, concentrations of selected toxic metals (Cd, Cu, Pb, Zn) of the apical part of *C. conicum* gametophyte were determined according to Esposito et al., 2018.

For both experiments, the Enrichment Factor (EF) was calculated as the ratio between the metal in the plant (mg g^{-1}) to the metal in the water (μg L^{-1}) (Ahmad et al., 2014).

2.5. Detection of ROS

A fluorescent technique using 2′-7′-dichlorofluorescein diacetate (DCFH-DA) has been used for quantitative measurement of ROS production according to Maresca et al. (2018). ROS quantity was monitored by fluorescence (excitation wavelength of 350 nm and emission wavelength of 600 nm).

2.6. Response to oxidative stress

Enzyme extraction and the determination of superoxide dismutase (SOD), catalase (CAT), and glutathione S-transferases (GST) activities were performed as reported in Maresca et al. (2018). Enzymes activity were calculated using commercial kits (SOD, CAT AND GST, Sigma-Aldrich Co., St Louis, MO, USA).

2.7. Reduced (GSH) and total and glutathione contents

The GSH and total glutathione contents of *C. conicum* were determined according to Salbitani et al. (2015) with minor adjustments. Specifically, 2 g of C. conicum were crushed in mortars with liquid nitrogen, and 4 mL of 5% sulfosalicylic acid were added to the powdered tissue. The homogenates were centrifuged at 12000g for 30 min at 4 °C. The extract was added to the reaction buffer containing 0.1-M Na-phosphate, pH 7.00, 1-mM of EDTA, 40 μL of 0.4% DTNB, and distilled water. The GSH and total glutathione contents were determined spectrophotometrically as previously described (Salbitani et a, 2015) and were expressed in μmol g^{-1} FW.

2.8. Total Phenolic Content (TPC) assay

The different *C. conicum* samples, dissolved in DMSO at 10 mg/mL concentration, were added at a final dose of 0.0625 − 0.5 mg/mL to a solution consisting of Folin-Ciocalteu reagent, 75 g/L Na2CO3, and water, in a 1:3:14 v/v/v ratio (Panzella et al., 2019). After 30 min incubation at 40 °C, the absorbance at 765 nm was measured. Gallic acid was used as a reference compound. Experiments were run in triplicate on each sample.

2.9. HPLC analysis

HPLC analysis was performed on the *in vitro* samples dissolved in methanol (5 mg/mL concentration) with an instrument equipped with a UV-Vis detector (Agilent, G1314A); a Phenomenex Sphereclone ODS column (250 × 4.60 mm, 5 μm) was used, at a flow rate of 1.0 mL/min; a 0.1% formic acid (solvent A)/methanol (solvent B) gradient elution was performed as follows: 5% B, 0–10 min; from 5% to 80% B, 10–47.5 min; the detection wavelength was 254 nm.

2.10. LC-MS analysis

LC-MS analyses were run on an Agilent LC-MS ESI-TOF 1260/6230DA instrument operating in positive ionization mode in the following conditions: nebulizer pressure 35 psig; drying gas (nitrogen) 5 L/min, 325 °C; capillary voltage 3500 V; fragmentor voltage 175 V. An Agilent Eclipse Plus C18 column, 150 × 4.6 mm, 5 μm at a flow rate of 0.4 mL/min was used, using the same eluant as above.

2.11. Confocal imaging

Samples treatment was done according to Maresca et al. (2020a). ROS were localized with the fluorescent probe 2′-7′ dichlorofluorescin diacetate (DCF-DA) solubilized in dimethyl sulphide DMSO and 10 mM Tris-HCl (pH 7.4), then dilute in MilliQ water to obtain a 25 μM staining solution. Thin thalli sections of *C.conicum* were then stained with 25 μM DCF-DA for 30 min. Stained sections were washed in Tris HCl (pH 7.4) for 10 min. Thalli sections were observed under a laser-scanning confocal microscope (Leica TCS SP5, Wetzlar, Germany) with an excitation wavelength of 476 nm and emission bandwidths 485/575 nm (green light), 610/685 nm (red light) (beginning-end).

GSH and thiol-peptides were localized with monochlorobimane (MCB) solubilized in DMSO and then in MilliQ water to obtain a 100 μM staining solution. Thin thalli sections of fresh *C. conicum* were stained with 100 μM MCB (Thermo Fisher Scientific, MA, USA) for 30 min at 21 °C in the dark, at near neutral pH conditions. After, observations were performed under a Leica TCS SP5 confocal laser scanning microscope (CLSM) with a 40X immersion objective. Excitation of MCB and chlorophyll was set at 405 nm wavelength, and emission detected at 460–520 nm (blue light) and 630–700 nm (red light) (beginning-end). Unstained *C.conicum* cross-sections were incubated into the same amount of DMSO solution without DCF-DA and MCB, and used as a negative control of DCF-DA and MCB. Three samples of *C.conicum* cross-sections thalli for each treatment and control condition were examined.

In both ROS and GSH and thiol peptides imaging, hardware settings, particularly detector gain and amplification offset, were adjusted to optimize fluorescence intensity in samples C, and the same values were kept with all samples to allow a semiquantitative comparison between different treatments. Data collection and processing were performed with the software LAS AF (Leica). Observations were repeated 3 times for each treatment.

2.12. Transmission electron microscopy

Collected samples, after thoroughly cleaning, were cut to pick subapical central parts of the thalli, about 3 mm below the apex, cutting away the wings. Protocol preparation for transmission electron microscopy (TEM) requires the following steps: overnight fixation at 4 °C with glutaraldehyde 2.5% (*v/v*) buffered solution (Sorenson's sodium phosphate buffer 0.025 M, pH 7.3), postfixation with 1% (*w/v*) osmium

tetroxide buffered solution, with the same buffer as before, added with KFeCN 0.8%, dehydration with alcohol up to propylene oxide, embedding in Spurr resin with subsequent polymerization at 70 °C in the oven. By ultramicrotomy, we obtained ultrathin 50 nm thick sections, which were collected on 300 mesh copper grids and stained with Uranyl Acetate Replacement stain (Electron Microscopy Science, Hatfield, PA, USA) and lead citrate. An EM208ES Philips TEM was employed for the observations. The observation was focused on photosynthetic parenchymata; three samples per treatment and 9 sections per sample were examined.

2.13. Statistical analysis

ROS production, SOD, CAT, GST activities, and glutathione contents were examined by one-way analysis of variance (ANOVA), followed by Tukey's multiple comparison post-hoc test. The student's t-test was performed on the results of the TPC assay. In all figures, values are presented as mean ± st. err; numbers not accompanied by the same letter are significantly different at $P < 0.05$. Data were analyzed using the software Statistica, version 7.0 (StatSoft, Tulsa, OK, USA). For the in-field and *in vitro* experiments, the relationships between bioaccumulation of heavy metals and biological responses were assessed using Pearson correlation analysis. Data from all sites (A, B, C) were analyzed together.

3. Results

3.1. Analytical determination of metal and EF in water samples and in liverwort

The concentrations of the heavy metals analyzed in the water (Table 1S) samples are very high and exceed the limits defined by Legislative Decree 172/2015 ("Implementation of Directive 2013/39 / EU, which amends Directives 2000/60 / EC about priority substances in the field of water policy"), especially for Cd and Pb (ref. 1 / A - Environmental quality standards in the water column and biota for substances on the priority list). Site C is affected by pressures due to the presence of ASI (Industrial Development Areas) zones, with industries subject to AIA (Integrated Environmental Authorization) (Fig. 1S).

As regards the bioaccumulation of heavy metals in the gametophyte of *C. conicum*, the detected concentrations reflect the concentrations of heavy metals measured in the selected sites (Table 1). Furthermore, for all the metals measured, a greater bioaccumulation capacity is noted in the *in vitro* samples compared to those in the field, probably due to a greater bioavailability of the metals in solution (Table 1).

Fig. 1 shows the EF for the considered heavy metals in the two experiments. In the field experiment, the EF of Cu (Fig. 1a) reached the highest value in C, whereas the lower EF occurred in B. In the *in vitro* conditions, EF increased when metals concentration increased (A>B>C). Looking at the differences between in-field and *in vitro* experiments, the in field experiment had the higher EF values (A in-field>A *in vitro*; B in field>B *in vitro*; C in field>C *in vitro*). For both Zn (Fig. 1b) and Cd (Fig. 1c), EF showed the same general pattern: as the metals concentration increase, EF increased in both field and *in vitro* experiments (A> B> C in field; A> B> C *in vitro*). For each level of metals concentration, the *in vitro* EF was higher relative to the field. In the field experiment, the EF of Pb (Fig. 1d) decreased from A to B, whereas the C presented an intermediate EF. On the other hand, *in vitro* experiment, the EF increased as metals concentration increased (A> B> C). Looking at the differences between in-field and *in vitro*, we highlighted that in the latter conditions the EF was tendentiously lower in respect to what was found in the field experiment. It is interesting to notice that EF values between in-field and *in vitro* are approximately equivalent, except for Cu and Pb *in vitro*.

3.2. ROS and oxidative stress response

In vitro experiments, the production of ROS in the samples follows an increasing trend, in fact in the samples of *C. conicum* exposed to the highest concentrations (samples C) of heavy metals a higher production of ROS is observed, also samples A and B have higher ROS values than the control if there is no statistically significant difference between the two. Regarding the enzymatic activity of CAT and SOD, an increase in the enzymatic activity is observed in samples B and C compared to the control even if there are no statistically significant differences between the two, in samples A the activity of both enzymes is greater than control but lower than samples B and C. The activity of the GST enzyme is higher in samples C, in samples A and B no significant differences are observed but the enzymatic activity is still higher than in the control (Fig. 2).

In field experiments, ROS production increases with increasing pollution of the three sites. As far as the enzymatic activity of SOD is concerned, an increase in the enzymatic activity is observed in samples B and C compared to the control even if there are no statistically significant differences between the two, in samples A the activity of SOD is greater than the control but lower than samples B and C. The activity of CAT and GST enzymes is greater in samples C, no significant differences are observed in samples A and B but the enzymatic activity is even greater than in the control (Fig. 2).

3.3. Glutathione contents in C. conicum in field and in vitro experiments

The total glutathione concentration increased in *C. conicum* exposed and collected in the three sites as previously described. Particularly, in samples B and C the values were significantly higher with respect to Ctrl and sample A. In the samples analyzed, both in the field and *in vitro* experiments, GSH contents were similar in Ctrl and A samples, while increased more significantly in C samples collected for in field experiments (Fig. 2). In the samples treated with a solution containing the same heavy metals concentration found in the three field sites (*in vitro* experiments), the same trend was observed: in B and C total glutathione was higher with respect to Ctrl and A samples (Fig. 2).

3.4. Phenolic content

To obtain information on the effects of exposure to heavy metals on the amounts of phenolic compounds in *C. conicum*, the Folin-Ciocalteu assay was performed on both the in-field and *in vitro* samples (Table 2). Notably, the highest TPC values were determined for *C. conicum* samples exposed to the highest concentrations of heavy metals (samples C). Moreover, an increasing trend in TPC was observed, with samples B showing a significantly higher value compared to samples A, although for these latter no significant differences with the *in*

Table 1
The concentration of metals (μg g^{-1}) in *C. conicum* exposed in field and *in vitro* experiments.

	Field			*In vitro*		
	A	**B**	**C**	**A**	**B**	**C**
Cu	22.582 ± 1.311^{a}	1340.643 ± 72.402^{b}	1098.201 ± 27.136^{c}	70.133 ± 2.019^{a}	1890.212 ± 10.727^{b}	2738.202 ± 70.198^{c}
Zn	156.763 ± 14.264^{a}	691.523 ± 4.013^{b}	1023.437 ± 71.465^{c}	90.434 ± 43.622^{a}	1562.329 ± 76.983^{b}	1965.441 ± 60.521^{c}
Cd	13.415 ± 1.053^{a}	161.223 ± 13.227^{b}	293.925 ± 23.812^{c}	19.112 ± 7.128^{a}	532.453 ± 32.112^{b}	982.812 ± 11.484^{c}
Pb	7.337 ± 0.999^{a}	70.422 ± 12.609^{b}	1064.113 ± 38.794^{c}	10.912 ± 1.621^{a}	47.894 ± 9.934^{b}	171.013 ± 4.544^{c}

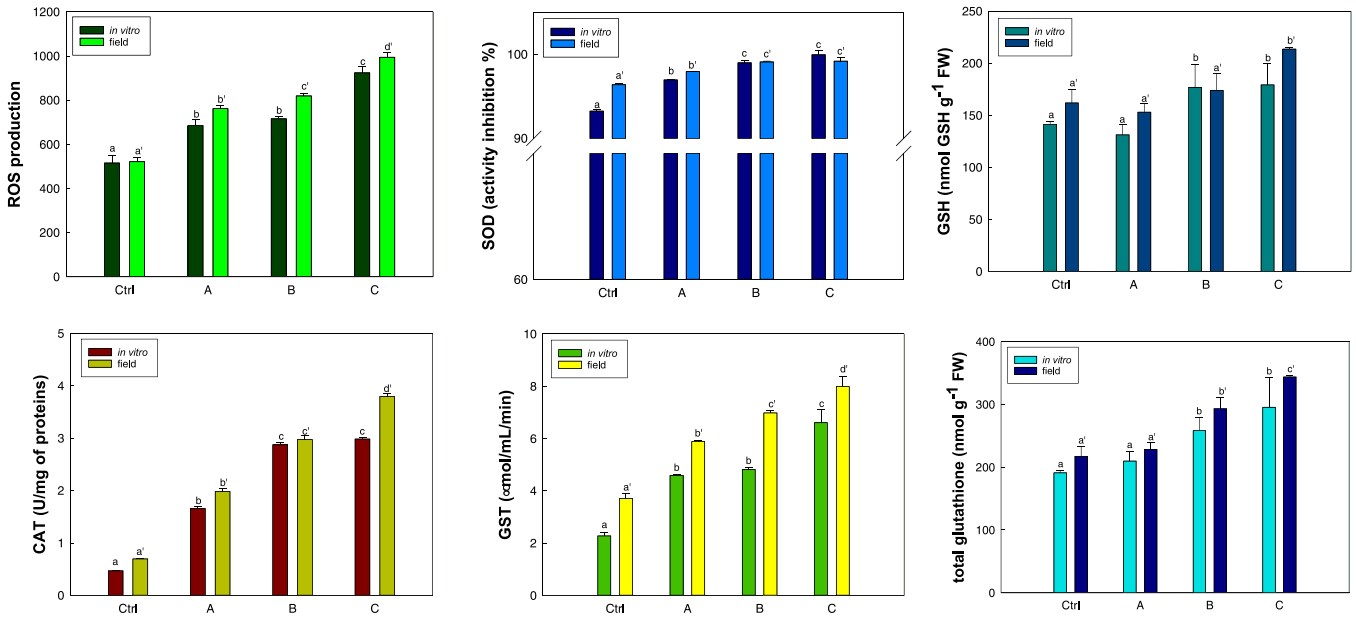

Fig. 2. ROS production (fluorescence intensity), antioxidant responses (SOD activity inhibition %, CAT, U/mg of protein, GST, μmol/mL/min), reduced glutathione (GSH, nmol g^{-1} FW) and total glutathione levels (nmol g^{-1} FW) in the samples A, B, C and control exposed in the field and *in vitro* experiments.

Table 2
TPC of *C. conicum* samples exposed to heavy metals in the field and *in vitro* experiments.

Sample	TPC (mg of gallic acid/mg of the sample)	
	Field	*in vitro*
A	0.039 ± 0.002a	0.0273 ± 0.0001a
B	0.065 ± 0.002b	0.0533 ± 0.0004b
C	0.085 ± 0.001c	0.0676 ± 0.0003c

vitro control (0.0288 ± 0.0005 mg of gallic acid/mg of the sample) were detected.

As shown in Fig. 2S, a very good linear correlation was found between the total concentration of metals determined by ICP-MS experiments and the TPC for both the in field and *in vitro* samples (R2 = 0.99 and 1.00, respectively), indicating that phenolic compound biosynthesis is closely related to the heavy metal exposure.

To gain information on the phenolic composition, the *C. conicum* samples exposed to the different heavy metals concentrations *in vitro* were dissolved in methanol and analyzed by HPLC. The elutographic profiles (Fig. 3) showed for all the samples the main compound eluted at *ca.* 41 min, whose concentration was found to increase moving from sample A to sample C, *i.e.* further to exposure to increasing concentration of heavy metals. Based on LC-MS analysis, showing pseudomolecular ion peaks [M+H]+, [M+Na]+, and [M+K]+ at *m/z* 259, 281, and 297, in that order, this compound was tentatively identified as

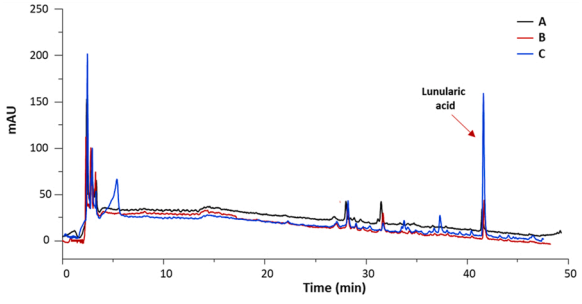

Fig. 3. HPLC profiles of *in vitro* A, B, and *C. conicum* samples.

lunularic acid, which has previously been reported as one of the main phenolic components of liverworts, including *C. conicum* (Abe and Ohta, 1984; Gorham, 1977; Pryce, 1971).

3.5. Confocal imaging

Under the chosen settings, confocal micrographs showed no DFC signal in both the field non-exposed control and in the *in vitro*-non-treated ones, where only red autofluorescence from chloroplasts was detected (Fig. 4). Green fluorescence related to ROS was detectable in all the field-exposed and *in vitro*-treated samples, with an increasing signal from samples A to C (Fig. 4). The red signal from chloroplasts was present in all the samples. ROS signal appeared patchy, marking unevenly the cell protoplast. In samples C, the peripheral cytoplasm and plasma membrane emit strong DFC signal (Fig. 4).

Under the steady settings, confocal micrographs showed faint MCB fluorescence from the field-non-exposed and *in vitro*-non-treated samples (controls), where red autofluorescence from chloroplasts was always detectable (Fig. 5). The signal from MCB increases from samples A to C, in both the field and *in vitro* experiment, and most of the blue signals seem to localize in vacuoles (Fig. 5).

3.6. Transmission electron microscopy

TEM observations showed that field-non-exposed and *in vitro*-non-treated control samples had the same ultrastructural appearance as samples A from both the field and *in vitro* experiments. Cells had a typical ultrastructure with a large central vacuole and, beneath the cell wall, typical oblong chloroplasts with well-developed thylakoids, arranged in grana and intergrana membranes, in a quite dense stroma. Inside chloroplasts starch grains and a few small dense plastoglobules are visible (Fig. 6a, f). The other organelles had also a typical appearance. Mitochondria had clear cristae in a dense stroma (Fig. 6b, g). The samples B from both the field and *in vitro* experiments had also a comparable appearance. Chloroplasts still maintained a well-developed thylakoid system, arranged in grana and intergra, and starch grains too. Large plastoglobules and thylakoid light swellings were developed. Mitochondria still had clear cristae and a dense stroma. (Fig. 6c, h). Samples C from both the field and *in vitro* experiments developed comparable ultrastructural changes compared to control samples.

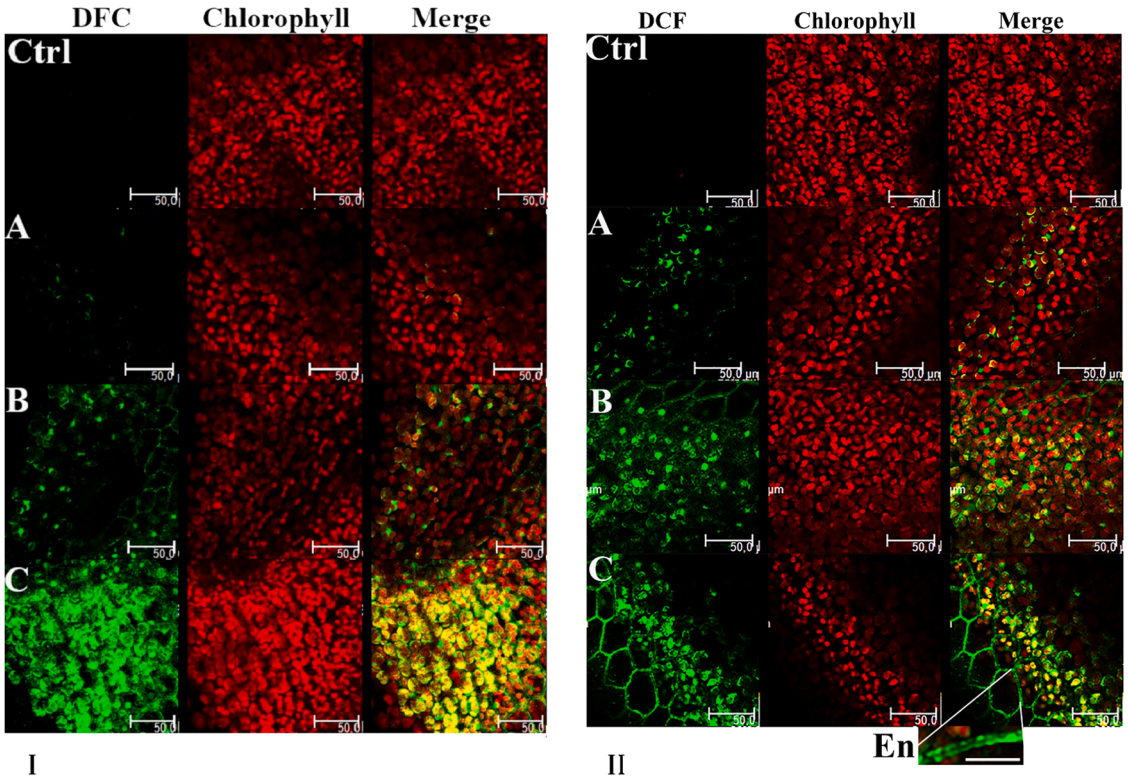

Fig. 4. Confocal laser scanning microscopy (CLSM) micrographs of the photosynthetic layer from the field-exposed (I) and *in vitro*-treated (II), DCF-DA-stained *C. conicum* samples A, B, C, and the non-exposed and non-treated one (control). The first column shows DCF signal, the second displays chloroplast autofluorescence and the third is the overlay. In the non-exposed and non-treated control sample, no DFC signal was detectable, while red chloroplast autofluorescence was well evident. In samples A, B, and C (in field and *in vitro*), DCF-signal, increasing from A to C, is visible from the cytoplasm and chloroplasts of the cells along with red autofluorescence from chloroplasts. (En) The micrograph is an enlargement of a detail from the C panel where a strong ROS signal from peripheral cytoplasm and plasma membrane is shown. Scale bars: Ctrl, A, B, C: 50 μ; En: 20 μ.

Chloroplasts appeared swollen and bulged, thylakoids developed swellings, stroma became electron clear (Fig. 6d, i). At some points, the outer membrane of the chloroplasts detached from the inner one, and multilamellar bodies were developed (Fig. 6e, j). Mitochondria showed crista remnants in a clear stroma (Fig. 6d).

3.7. Pearson's correlation

Table 2S shows the Pearson correlation; data collected for in the field and *in vitro* experiment were pooled together and the correlation between the bioaccumulation of heavy metals and biological responses were derived. All biological responses resulted directly correlated with the concentration of all metals measured, and all metals were directly intercorrelated.

4. Discussion

In this work, the biological responses of the liverwort *C. conicum* to heavy metal pollution of freshwater was reported. The ability of the liverwort *C. conicum* to bioaccumulate heavy metals in both in field and *in vitro* experiments was tested. Furthermore, its tolerance was assessed through several functional and structural indicators. Heavy metal bioaccumulations in C. conicum varied notably among the three in field sites, linearly with the concentrations found in water samples. This results are consistent with those from Maresca et al. (2018).

For the first time, a study is conducted that takes into consideration a wide range of antioxidant responses, from the activation of enzymes to the response *via* glutathione to the synthesis of molecules to counteract the increase of ROS. Furthermore, for the first time, ROS and thiol compounds cellular localization is identified. Furthermore, antioxidant responses of *C. conicum* are compared both in environmental conditions and *in vitro* in order to reduce confounding variables and to have responses that can only be compared with the concentrations of the metals detected at the 3 exposure sites in the field. As evidenced by the present results, heavy metals exposure implies ROS generation that trigger several antioxidant responses in *C. conicum*. In fact, ROS content is strongly correlated with the antioxidant activities of SOD, CAT and GST. As regards the production of ROS, they are also present at low concentrations of heavy metals, that is, both in the control and in the treated samples. These results are consistent with the idea that ROS are not only produced as a response to abiotic and biotic stresses, but they support biological processes such as cellular proliferation, physiological functions, and viability, thus being essential for plants (Mittler, 2017). Moreover, it is well known that heavy metals cause unbalances in redox homeostasis in plants, inducing the accumulations of ROS such as superoxide anion, hydroxyl radicals, and hydrogen peroxide.

These results agree with those obtained on another bryophyte: in the liverwort *Lunularia cruciata* collected in different urban and country sites and *in vitro* tests, the activity of antioxidant enzymes was related to the presence of heavy metals and production and localization of reactive oxygen species (Maresca et al., 2020a); The moss *L. riparium* exposed in the same Regi Lagni sites showed the biological responses to ROS activating the antioxidant enzymes (Maresca et al., 2018). All these responses were consistent with the degree of pollution of sites.

It is known that the tripeptide glutathione (γ-Glu-Cys-Gly) is involved in the response of plants to environmental stress such as heavy metal exposure (Carfagna et al., 2011, 2021; Asgher et al., 2017). Furthermore, the balance between reduced and oxidized forms of glutathione (GSH and GSSG) may be implied in the regulation of stress-related marker genes at the transcriptional level. The total

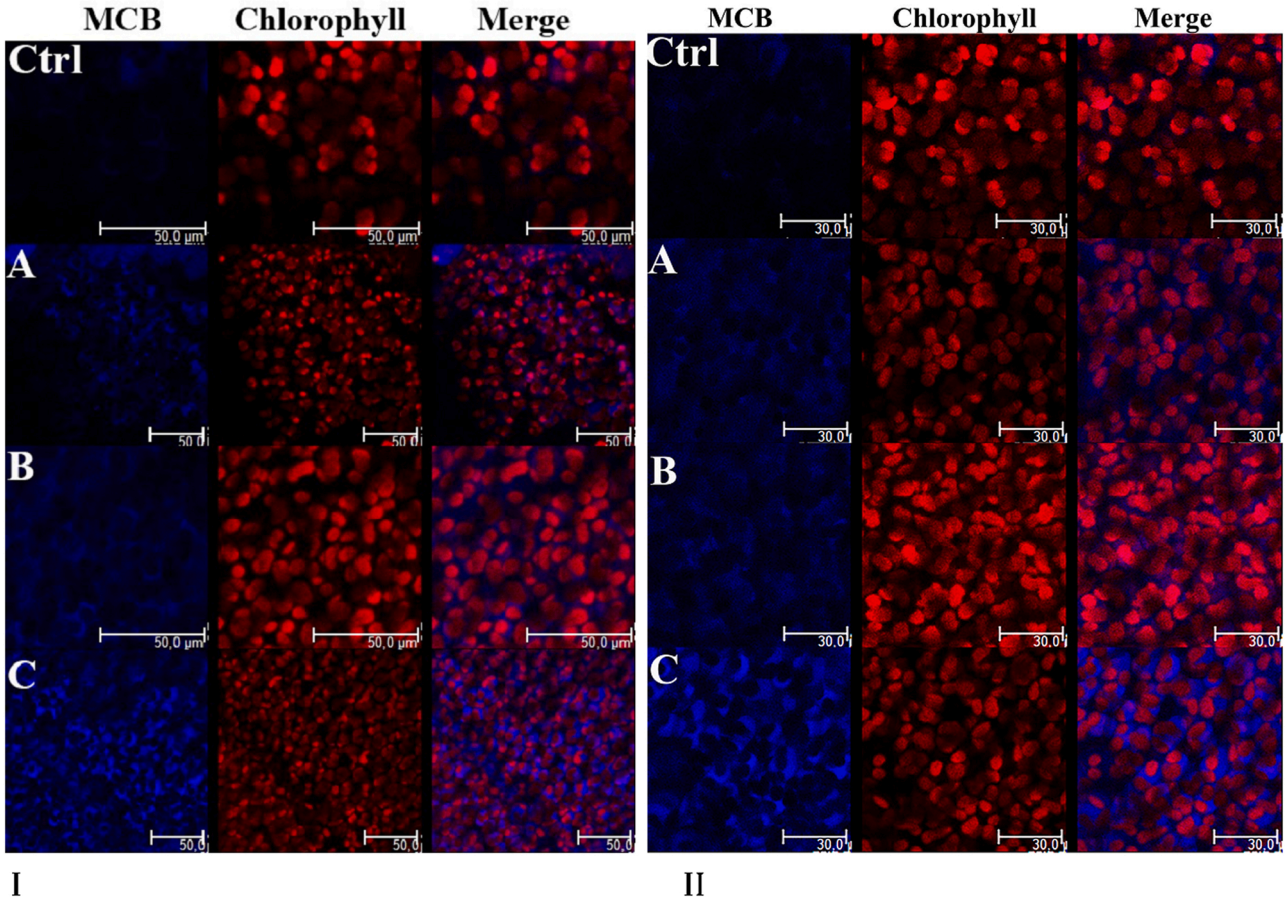

Fig. 5. Confocal laser scanning microscopy (CLSM) micrographs of the photosynthetic layer of thalli from the field-exposed and the *in vitro*-treated, MCB-stained *C. conicum* samples A, B, C, and the non-exposed and non-treated one (control). The first column shows the MCB signal, the second displays chlorophyll autofluorescence and the third is the overlay. MBC signal, increasing from the non-exposed and non-treated control to samples C, is detectable in the cytoplasm of the cells along with autofluorescence from chloroplasts. Scale bars: CTRL, A, B, C: 30 µ.

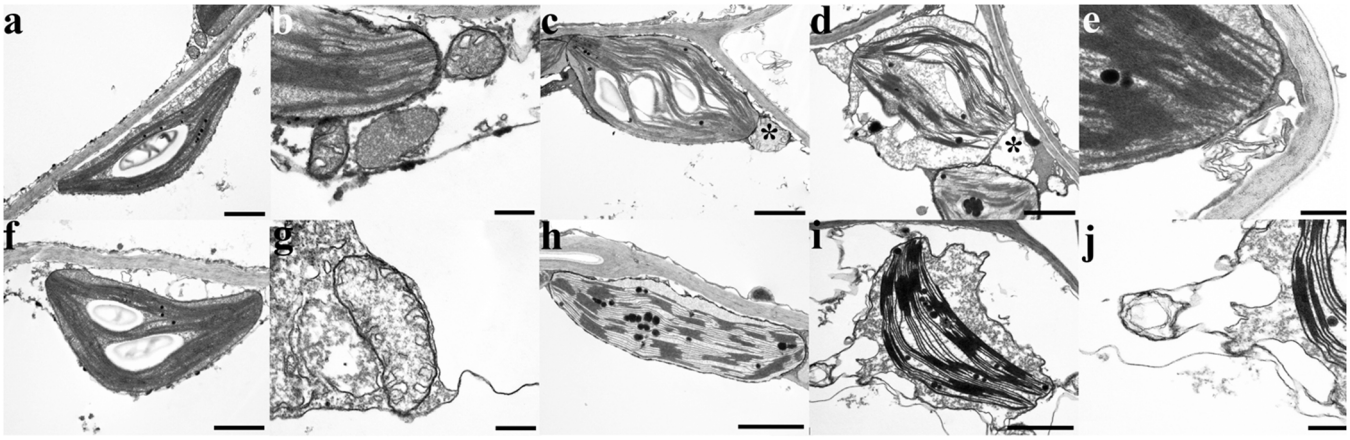

Fig. 6. Fig. shows TEM micrographs of *C. conicum* samples after field (Figs. a-e) and *in vitro* (Figs. f-j) treatments. Figs. a-b. Field sample A. Fig a shows, beneath the cell wall, a typical lenticular chloroplast with well-developed thylakoids, arranged in grana and intergrana membranes, in a quite dense stroma, where a central starch grain and a few small dense plastoglobules are present. Fig. b. Two mitochondria with clear cristae in a dense stroma and peroxisome next to a chloroplast. Fig. c. Field sample B. An oblong chloroplast with a well-developed thylakoid system, starch grains, and a few thylakoids. Some of the thylakoids developed swellings. Next to the chloroplast is a mitochondrion with clear cristae in a quite dense stroma (asterisk). Figs. d-e. Field sample C. Fig. d. An altered swollen chloroplast where thylakoids developed large swellings and the stroma appears rather clear. A mitochondrion with crista remnants and clear stroma (asterisk). Fig. e. Beneath the cell wall, next to a chloroplast, is a multilamellar body. Fig f-g. *In vitro* sample, A. Fig. f shows an oblong chloroplast with a typical appearance, where a well-developed thylakoid system, arranged in grana and intergrana, is in a dense stroma. Two starch grains and a few plastoglobules are present. Fig. g. A mitochondrion with clear cristae in a dense stroma. Fig. h. An oblong chloroplast with grana and intergrana arrangement of thylakoids is well visible. Large dense plastoglobules are also visible. Fig. i. An altered swollen and bulged chloroplast where the well-developed thylakoids system is in a clear abundant stroma. Fig. j. Detail of fig. i. Severe swelling of the chloroplast outer membrane, which detached from the inner one at some points, leaving large spaces. Scale bars: 1 µ (a, c, d, f, h, i), 300 nm (b, e, g, j).

glutathione content increase in *C. conicum* in field and *in vitro* experiments suggesting a major stressful environmental impact in samples from the sites of Acerra and Castel Volturno (B and C). The total and reduced form of glutathione, GSH, significantly increased in *C. conicum* samples collected in Castelvolturno (C) may have protected the liverwort from heavy metal pollution and not only, since the concentration of glutathione increased but to a minor extent in samples from *in vitro* experiments, where the only abiotic stress considered was relative to the exposition to high heavy metals concentrations. Notably, an increase in phenolic compound biosynthesis was also observed further exposure of *C. conicum* to heavy metals both in field and *in vitro* experiments, with a very good correlation between TPC values and heavy metal concentrations. This is well in line with what was previously reported in several plants in the case of heavy metal-induced toxicity (Keziah et al., 2016; Manjunath and Reddy, 2019; Rohani et al., 2019; Kapoor et al., 2016).

As for the localization of ROS, under the fixed imaging settings of our confocal microscopy, both the field non-exposed samples and *in vitro* non-treated samples did not show any green DCF signal but only red autofluorescence from chloroplasts referrable to chlorophyll. That suggests that the ROS amount was under detection at least. In both the field-exposed and *in vitro*-treated samples, the green DFC signal increased from A to C, showing an increasing presence of ROS. The finding is consistent with our chemical data, demonstrating ROS amount being lowest in the field non-exposed and *in vitro* non-treated control samples and highest in C ones from both the experiments. DCF-DA enters the cells where it undergoes cleavage by cytoplasm esterases. The de-esterificated derivative stays inside the cytoplasm compartments and is not able to cross membranes due to negatively charging. The esterificated DFC-DA is not able to give significant fluorescence to effectively detect ROS; conversely, only the de-esterificated forms give fluorescence after oxidation. So, the DCF signal marks ROS inside cell compartments and allows their localization inside the cell. (Sandalio et al., 2008; Kristiansen et al., 2009). In our exposed and treated samples, ROS distribution appears patchy, according to other studies on plants demonstrating a ROS localization inside specific organelles, such as nuclei, mitochondria, peroxisomes, chloroplasts, and plasma membranes rather than an even distribution inside the protoplast (Kristiansen et al., 2009). In samples C, enlargement of external protoplast and cell wall images reveals that peripheral cytoplasm and cell membrane emit a strong uneven signal, giving the appearance of emitting cell walls at low magnification. On the whole, our findings are comparable to another study on the same species exposed to Cd stress, where, in the untreated samples, no DFC signal was detected and ROS fluorescence of the treated ones was patchy in the protoplast and related to the amount of Cd supplied to the plants (Maresca et al., 2020b).

As for localization of SH groups, under the chosen imaging settings, confocal micrographs of MCB-labeled samples showed faint signal from the field non-exposed and *in vitro* non-treated samples, whereas the fluorescence from thiol peptides was well visible in all the exposed and treated samples, with an increasing trend from A- to C specimens. That suggests the thiol peptide amount was lower in the control samples and their amount was related to the induced stress in the other specimens, accordingly with the chemical data. Most of the signal seems to localize in vacuoles. Those findings are in agreement with another study on *C. conicum* exposed to Cd stress, where comparable results were obtained with 2 different Cd concentrations (Maresca et al., 2020b).

TEM observations showed that samples A from both the field and *in vitro* experiments have a typical ultrastructure, which demonstrates that both exposures in site A and *in vitro* treatment with solution A did not impair cell ultrastructure. Samples B from both the experiments developed comparable light alterations, the ultrastructure being mostly preserved. Differently, samples C from both the experiments developed severe alterations with swelling of the whole chloroplasts and the thylakoids inside, with the outer membrane sometimes detaching from the inner one. Swelling and shrinkage of the whole cell or single organelles and membrane compartments, in general, is supposed to be caused by the loss of selective permeability control of membranes. That, in turn, depends either on direct damage to the membrane or on an energy depletion (Schwartzman and Cidlowski, 1993). If selective permeability is impaired, ions move across the membrane downstream concentration gradients, and the shifted water cause swelling or shrinkage of membrane compartments (Schwartzman and Cidlowski, 1993). In addition, ROS are a well-known cause of damage to membranes due to lipid peroxidation (Su et al., 2019). Furthermore, our finding of severe swelling phenomena in chloroplasts and thylakoids associated with mitochondria showing only crista remnants and clear stroma, evident signs of severe ultrastructure damage, suggests that energy depletion could also play a role in the development of those ultrastructure features.

Samples C from both experiments developed multilamellar bodies (MLBs). Those are membrane-bound cellular structures, composed of concentric membrane layers, related to autophagic phenomena. Degradative autophagic vacuoles arise after acquiring lysosomal features from nascent, immature autophagic vacuoles, which feature multiple limiting membranes and are regarded to form by the sequestration of cytoplasm by smooth endoplasmic reticulum membranes (Hariri et al., 2000). Multilamellar bodies (MLBs) are formed by the parallel apposition of lipid membranes from the endoplasmic reticulum encircling portions of cytoplasm; the lysosomal nature of the MLB has been demonstrated by the localization of various lysosomal enzymes to this organelle (Hariri et al., 2000). Furthermore, stress stimulates autophagy, which is useful to recycle and degrade damaged cell components (Bassham, 2009; Hayward et al., 2009) and ROS have also been demonstrated to enhance autophagocytosis phenomena through lipid peroxidation (Su et al., 2019).

In particular, from our data, it is clear that all the stress alterations caused by heavy metal pollution are strongly correlated with the concentrations of pollutants detected in the environment or supplied *in vitro*. This leads us to hypothesize their possible use as pollution biomarkers as all the biological responses considered show a trend consistent with the degree of pollution of the sites. Furthermore, this study confirms the ability of the liverwort *C. conicum* to respond to heavy metal pollution in a manner consistent with the degree of pollution and therefore with the possibility of considering it a good bioindicator of environmental pollution both in urban sites (Basile et al., 2013) and aquatic environments.

5. Conclusions

The present study showed the ability of *C. conicum* as bioaccumulator of heavy metals, combining field and *in vitro* experiments, verifying its tolerance through several structural and functional indicators; the biological responses considered, ROS production and localization, antioxidant enzymes, glutathione (reduced and oxidized) levels, phenolic content, ultrastructural damage and localization of compounds presenting thiol groups responded consistently with the expected environmental stress and were related to the concentrations of the most toxic metals found in the soil and bioaccumulated in liverwort. Based on the present results, we can conclude that not only higher but also lower plants (bryophytes) can be used as an alternative first-tier assay system for the detection of environmental pollution.

The combination of field and *in vitro* experiments has shown that *C. conicum* can be used as an excellent bioindicator and bioaccumulator in sites highly polluted by human activity, given its reactivity and resistance to heavy metals.

Funding

"This study received no external funding".

CRediT authorship contribution statement

Adriana Basile, **Federica Carraturo, Lucia Panzella, Viviana Maresca, Simona Carfagna**: Conceptualization, Validation, Supervision. **Federica Moccia**, **Giovanna Salbitani, Viviana Maresca**: Methodology, Formal analysis. **Federica Moccia, Marilena Insolvibile, Piergiorgio Cianciullo, Sergio Sorbo**: Investigation. **Adriana Basile, Lucia Panzella, Piergiorgio Cianciullo, Simona Carfagna, Viviana Maresca**: Writing – original draft preparation.

Declaration of Competing Interest

The authors declare that they have no known competing financial interests or personal relationships that could have appeared to influence the work reported in this paper.

Appendix A. Supporting information

Supplementary data associated with this article can be found in the online version at doi:10.1016/j.ecoenv.2022.113365.

References

Abe, S., Ohta, Y., 1984. The concentrations of lunularic acid and prelunularic acid in liverworts. Phytochemistry 23, 1379–1381. https://doi.org/10.1016/S0031-9422(00)80469-0.

Ahmad, S.S., Reshi, Z.A., Shah, M.A., Rashid, I., Ara, R., Andrabi, S.M.A., 2014. Phytoremediation Potential of Phragmites australis in Hokersar Wetland - A Ramsar Site of Kashmir Himalaya. Int. J. Phytoremediat. 16, 1183–1191. https://doi.org/10.1080/15226514.2013.821449.

Asgher, M., Per, T.S., Anjum, S., Khan, M.I.R., Masood, A., Verma, S., Khan, N.A., 2017. Contribution of glutathione in heavy metal stress tolerance in plants. In: Khan, M.I. R., Khan, N.A. (Eds.), Reactive Oxygen Species and Antioxidant Systems in Plants: Role and Regulation under Abiotic Stress. Springer, Singapore, pp. 297–313. https://doi.org/10.1007/978-981-10-5254-5_12.

Basile, A., Sorbo, S., Aprile, G., Conte, B., Castaldo Cobianchi, R., Pisani, T., Loppi, S., 2009. Heavy metal deposition in the Italian "triangle of death" determined with the moss Scorpiurum circinatum. Environ. Pollut. 157, 2255–2260. https://doi.org/10.1016/j.envpol.2009.04.001.

Basile, A., Sorbo, S., Conte, B., Cardi, M., Esposito, S., 2013. Ultrastructural changes and Heat Shock Proteins 70 induced by atmospheric pollution are similar to the effects observed under in vitro heavy metals stress in Conocephalum conicum (Marchantiales–Bryophyta). Environ. Pollut. 182, 209–216. https://doi.org/10.1016/j.envpol.2013.07.014.

Bassham, D.C., 2009. Function and regulation of macroautophagy in plants. Biochimica et Biophysica Acta (BBA) - Molecular Cell Research. Autophagy 1793, 1397–1403. https://doi.org/10.1016/j.bbamcr.2009.01.001.

Bove, M.A., Ayuso, R.A., De Vivo, B., Lima, A., Albanese, S., 2011. Geochemical and isotopic study of soils and waters from an Italian contaminated site: Agro Aversano (Campania). J. Geochem. Explor. 109, 38–50. https://doi.org/10.1016/j.gexplo.2010.09.013.

Carfagna, S., Salbitani, G., Innangi, M., Menale, B., De Castro, O., Di Martino, C., Crawford, T.W., 2021. Simultaneous Biochemical and Physiological Responses of the Roots and Leaves of Pancratium maritimum (Amaryllidaceae) to Mild Salt Stress. Plants (Basel) 10, 345. https://doi.org/10.3390/plants10020345.

Carfagna, S., Vona, V., Salbitani, G., Sorbo, S., Lanza, N., Conte, B., Di Martino Rigano, V., Cobianchi, R.C., Golia, B., Basile, A., 2011. Cysteine synthesis in Scorpiurum circinatum as a suitable biomarker in air pollution monitoring. Int. J. Environ. Health 5, 93–105. https://doi.org/10.1504/IJENVH.2011.039859.

di Martino, D., 2014, Ecologie dell'inquinamento Progetto di territorio attraverso la bonifica [doctoral dissertation]. ⟨http://www.fedoa.unina.it/10025/⟩.

Esposito, S., Sorbo, S., Conte, B., Basile, A., 2012. Effects of heavy metals on ultrastructure and HSP70S induction in the aquatic moss Leptodictyum riparium Hedw. Int. J. Phytoremediat. 14, 443–455. https://doi.org/10.1080/15226514.2011.620904.

Gorham, J., 1977. Metabolism of lunularic acid in liverworts. Phytochemistry 16, 915–918. https://doi.org/10.1016/S0031-9422(00)86692-3.

Grezzi, G., Ayuso, R.A., De Vivo, B., Lima, A., Albanese, S., 2011. Lead isotopes in soils and groundwaters as tracers of the impact of human activities on the surface environment: The Domizio-Flegreo Littoral (Italy) case study. J. Geochem. Explor., Pedogeochem. Mapp. Potential. Toxic. Elem. 109, 51–58. https://doi.org/10.1016/j.gexplo.2010.09.012.

Hariri, M., Millane, G., Guimond, M.-P., Guay, G., Dennis, J.W., Nabi, I.R., 2000. Biogenesis of multilamellar bodies via autophagy. Mol. Biol. Cell 11, 255–268.

Hayward, A.P., Tsao, J., Dinesh-Kumar, S.P., 2009. Autophagy and plant innate immunity: Defense through degradation. Semin. Cell Dev. Biol., Syst. Biol. Plant-Pathog. Interact. 20, 1041–1047. https://doi.org/10.1016/j.semcdb.2009.04.012.

Kapoor, D., Rattan, A., Bhardwaj, R., Kaur, S., Gupta Manoj, A., 2016. Antioxidative defense responses and activation of phenolic compounds in Brassica juncea plants exposed to cadmium stress. Int. J. Green. Pharm. 10, 228–234.

Kelly, M.G., Girton, C., Whitton, B.A., 1987. Use of moss-bags for monitoring heavy metals in rivers. Water Res 21, 1429–1435. https://doi.org/10.1016/0043-1354(87)90019-4.

Keziah, J.E.J., Sharmila, S., Rebecca, L.J., 2016. Effect of heavy metals and UV irradiation on the production of flavonoids in Indigofera tinctoria. Int. J. Pharm. Sci. Rev. Res. 39, 104–107.

Kristiansen, K.A., Jensen, P.E., Møller, I.M., Schulz, A., 2009. Monitoring reactive oxygen species formation and localisation in living cells by use of the fluorescent probe CM-H(2)DCFDA and confocal laser microscopy. Physiol. Plant 136, 369–383. https://doi.org/10.1111/j.1399-3054.2009.01243.x.

Maresca, V., Fusaro, L., Sorbo, S., Siciliano, A., Loppi, S., Paoli, L., Monaci, F., Karam, E. A., Piscopo, M., Guida, M., Galdiero, E., Insolvibile, M., Basile, A., 2018. Functional and structural biomarkers to monitor heavy metal pollution of one of the most contaminated freshwater sites in Southern Europe. Ecotoxicol. Environ. Saf. 163, 665–673. https://doi.org/10.1016/j.ecoenv.2018.07.122.

Maresca, V., Lettieri, G., Sorbo, S., Piscopo, M., Basile, A., 2020a. Biological Responses to Cadmium Stress in Liverwort Conocephalum conicum (Marchantiales). Int. J. M. Sci. 21, 6485. https://doi.org/10.3390/ijms21186485.

Maresca, V., Sorbo, S., Loppi, S., Funaro, F., Del Prete, D., Basile, A., 2020b. Biological effects from environmental pollution by toxic metals in the "land of fires" (Italy) assessed using the biomonitor species Lunularia cruciata L. (Dum). Environ. Pollut. 265, 115000 https://doi.org/10.1016/j.envpol.2020.115000.

Mittler, R., 2017. ROS are good. Trends Plant Sci. 22, 11–19. https://doi.org/10.1016/j.tplants.2016.08.002.

Manjunath, B., Reddy, J., 2019. Comparative evaluation of air pollution tolerance of plants from polluted and non-polluted regions of Bengaluru. J. Appl. Biol. 7, 63–68.

Panzella, L., Moccia, F., Toscanesi, M., Trifuoggi, M., Giovando, S., Napolitano, A., 2019. Exhausted woods from tannin extraction as an unexplored waste biomass: Evaluation of the antioxidant and pollutant adsorption properties and activating effects of hydrolytic treatments. Antioxidants 8. https://doi.org/10.3390/antiox8040084.

Pryce, R.J., 1971. Lunularic acid, a common endogenous growth inhibitor of liverworts. Planta 97, 354–357. https://doi.org/10.1007/BF00390214.

Rohani, N., Daneshmand, F., Vaziri, A., Mahmoudi, M., Saber-Mahani, F., 2019. Growth and some physiological characteristics of Pistacia vera L. cv Ahmad Aghaei in response to cadmium stress and Glomus mosseae symbiosis. S. Afr. J. Bot. 124, 499–507. https://doi.org/10.1016/j.sajb.2019.06.001.

Salbitani, G., Vona, V., Bottone, C., Petriccione, M., Carfagna, S., 2015. Sulfur deprivation results in oxidative perturbation in Chlorella sorokiniana (211/8k). Plant Cell Physiol. 56, 897–905. https://doi.org/10.1093/pcp/pcv015.

Sandalio, L.M., Rodríguez-Serrano, M., Romero-Puertas, M.C., Del Río, L.A., 2008. Imaging of reactive oxygen species and nitric oxide in vivo in plant tissues. Methods Enzym. 440, 397–409. https://doi.org/10.1016/S0076-6879(07)00825-7.

Schwartzman, R.A., Cidlowski, J.A., 1993. Apoptosis: the biochemistry and molecular biology of programmed cell death*. Endocr. Rev. 14, 133–151. https://doi.org/10.1210/edrv-14-2-133.

Senior, K., Mazza, A., 2004. Italian "Triangle of death" linked to waste crisis. Lancet Oncol. 5, 525–527. https://doi.org/10.1016/s1470-2045(04)01561-x.

Sorbo, S., Aprile, G., Strumia, S., Castaldo Cobianchi, R., Leone, A., Basile, A., 2008. Trace element accumulation in Pseudevernia furfuracea (L.) Zopf exposed in Italy's so called Triangle of Death. Sci. Total Environ. 407, 647–654. https://doi.org/10.1016/j.scitotenv.2008.07.071.

Su, L.-J., Zhang, J.-H., Gomez, H., Murugan, R., Hong, X., Xu, D., Jiang, F., Peng, Z.-Y., 2019. Reactive oxygen species-induced lipid peroxidation in apoptosis, autophagy, and ferroptosis. Oxid. Med. Cell. Longev. 2019, 5080843. https://doi.org/10.1155/2019/5080843.